



## RESEARCH ARTICLE

# Noninvasive quantitative evaluation of viable islet grafts using $^{111}\text{In}$ -exendin-4 SPECT/CT

Ainur Botagarova<sup>1</sup>  | Takaaki Murakami<sup>1</sup>  | Hiroyuki Fujimoto<sup>2</sup> |  
Muhammad Fauzi<sup>1</sup> | Sakura Kiyobayashi<sup>1</sup> | Daisuke Otani<sup>1</sup> | Nanae Fujimoto<sup>3</sup> |  
Nobuya Inagaki<sup>1,4</sup>

<sup>1</sup>Department of Diabetes, Endocrinology and Nutrition, Graduate School of Medicine, Kyoto University, Kyoto, Japan

<sup>2</sup>Radioisotope Research Center, Agency for Health, Safety and Environment, Kyoto University, Kyoto, Japan

<sup>3</sup>Department of Regeneration Science and Engineering Laboratory of Experimental Immunology, Institute for Life and Medical Sciences, Kyoto University, Kyoto, Japan

<sup>4</sup>Medical Research Institute KITANO HOSPITAL, PIIF Tazuke-kofukai, Osaka, Japan

## Correspondence

Nobuya Inagaki, Department of Diabetes, Endocrinology and Nutrition, Graduate School of Medicine, Kyoto University, 54 Kawahara-cho, Shogoin, Sakyo-ku, Kyoto 606-8507, Japan.  
Email: [inagaki@kuhp.kyoto-u.ac.jp](mailto:inagaki@kuhp.kyoto-u.ac.jp)

## Funding information

Japan Association for Diabetes Education and Care (JADEC); Japan Diabetes Foundation; Japan Foundation for Applied Enzymology; Japan IDDM network; MEXT | Japan Society for the Promotion of Science (JSPS), Grant/Award Number: 21K20931, 22K16411 and 21K08553; Ministry of Education, Culture, Sports, Science and Technology (MEXT)

## Abstract

Islet transplantation (IT) is an effective  $\beta$ -cell replacement therapy for patients with type 1 diabetes; however, the lack of methods to detect islet grafts and evaluate their  $\beta$ -cell mass (BCM) has limited the further optimization of IT protocols. Therefore, the development of noninvasive  $\beta$ -cell imaging is required. In this study, we investigated the utility of the  $^{111}\text{In}$ -labeled exendin-4 probe  $\{[\text{Lys}^{12}(\text{111In-BnDTPA-Ahx})\text{exendin-4}]\}$  ( $^{111}\text{In}$  exendin-4) to evaluate islet graft BCM after intraportal IT. The probe was cultured with various numbers of isolated islets. Streptozotocin-induced diabetic mice were intraportally transplanted with 150 or 400 syngeneic islets. After a 6-week observation following IT, the ex-vivo liver graft uptake of  $^{111}\text{In}$ -exendin-4 was compared with the liver insulin content. In addition, the in-vivo liver graft uptake of  $^{111}\text{In}$  exendin-4 using SPECT/CT was compared with that of liver graft BCM measured by a histological method. As a result, probe accumulation was significantly correlated with islet numbers. The ex-vivo liver graft uptake in the 400-islet-transplanted group was significantly higher than that in the control and the 150-islet-transplanted groups, consistent with glycemic control and liver insulin content. In conclusion, in-vivo SPECT/CT displayed liver islet grafts, and uptakes were corroborated by histological liver

**Abbreviations:**  $^{111}\text{In}$ , indium 111; Ahx, 6-aminohexanoic acid; AUC, area under the curve; BCM,  $\beta$ -cell mass; BnDTPA, isothiocyanate-benzyl-DTPA; GLP-1R, glucagon-like peptide-1 receptor; IPGTT, intraperitoneal glucose tolerance test; IT, islet transplantation; MRI, magnetic resonance imaging; PET, positron emission tomography; RI, radioactive isotope; SPECT/CT, single-photon emission computed tomography/computed tomography; T-PER, tissue protein extraction reagent; %ID/g, percentage of injected dose per gram of tissue.

Ainur Botagarova and Takaaki Murakami have contributed equally to this work.

This is an open access article under the terms of the [Creative Commons Attribution-NonCommercial](https://creativecommons.org/licenses/by-nc/4.0/) License, which permits use, distribution and reproduction in any medium, provided the original work is properly cited and is not used for commercial purposes.

© 2023 The Authors. *The FASEB Journal* published by Wiley Periodicals LLC on behalf of Federation of American Societies for Experimental Biology.

BCM.  $^{111}\text{In}$ -exendin-4 SPECT/CT can be used to visualize and evaluate liver islet grafts noninvasively after intraportal IT.

#### KEYWORDS

$\beta$ -cell mass,  $\beta$ -cell imaging, islet transplantation, type 1 diabetes mellitus, SPECT/CT

## 1 | INTRODUCTION

Loss of  $\beta$ -cell mass (BCM) is an important factor in the development and progression of diabetes mellitus.<sup>1</sup> In type 1 diabetes, a substantial  $\beta$ -cell loss is observed because of autoimmune destruction, which results in a constant need for insulin replacement therapy.<sup>2</sup>  $\beta$ -cell replacement therapy, such as pancreatic islet transplantation (IT) via the portal vein, represents a promising method for achieving BCM restoration and glycemic stability with or without a reduced insulin requirement.<sup>3,4</sup> Although the current method has yielded favorable outcomes for IT, only 32% and 8% of patients remained insulin independent 5 and 20 years later, respectively.<sup>5,6</sup> In addition, repeated ITs are required to maintain a certain level of BCM for maintaining an insulin-independent status.<sup>7-9</sup> Thus, real-time monitoring of islet graft BCM in patients receiving IT could provide useful information for a deeper understanding of the fate of islet grafts and will enable the optimization of IT protocols to improve the clinical outcomes.<sup>3</sup> Current practical methods for monitoring viable islet grafts rely on functional tests such as measurement of plasma insulin or C-peptide levels<sup>10</sup>; however, these tests do not reflect islet graft function or BCM directly but are influenced by destruction of islet grafts.<sup>11,12</sup> Therefore, developing a noninvasive  $\beta$ -cell imaging technology which enables the evaluation of islet graft BCM would be advantageous.<sup>3,13-15</sup>

Various  $\beta$ -cell imaging techniques to assess BCM, including islet grafts, have been evaluated over the last few decades<sup>12-14</sup>; however, the clinical application remains challenging. Recently, exendin-based glucagon-like peptide-1 receptor (GLP-1R)-targeted imaging has emerged as a promising noninvasive  $\beta$ -cell imaging technique.<sup>13-15</sup> In particular, a  $^{111}\text{In}$ -labeled exendin-4 derivative {[Lys12( $^{111}\text{In}$ -BnDTPA-Ahx)]exendin-4} ( $^{111}\text{In}$ -exendin-4) has been used for the noninvasive longitudinal evaluation of pancreatic BCM in different mouse models.<sup>14,16-21</sup> In the  $^{111}\text{In}$ -exendin-4 SPECT/CT images, the radioactive isotope (RI) uptake into the pancreas is significantly correlated with histologically measured BCM,<sup>17-20</sup> suggesting that  $^{111}\text{In}$ -exendin-4 may be useful for the assessment of islet graft BCM as well as pancreatic BCM. However, the utility of GLP-1R-targeted imaging has not been fully evaluated with respect to islet grafts,

especially in intraportal transplantation, which is currently the only practical IT method available in clinical settings. Therefore, in this study, we investigated the feasibility of  $^{111}\text{In}$ -exendin-4 SPECT/CT for the noninvasive visualization of islet grafts and evaluated BCM in diabetic mice receiving intraportal syngeneic IT.

## 2 | MATERIALS AND METHODS

### 2.1 | Animals

Male C57BL/6JJmsSlc mice (Japan SLC, Inc., Shizuoka, Japan) aged 8–10 weeks served as recipients and donors for syngeneic ITs. The mice were given free access to standard rodent chow and water and were housed in a temperature-controlled environment with a 14:10-h light/dark cycle. The animal care and protocols were reviewed and approved by the Kyoto University Graduate School of Medicine Animal Care and Use Committee (approval no. MedKyo 21508, 22222, 22227). Recipient animals were rendered diabetic by a single intraperitoneal injection of streptozotocin (catalog no. 197-15153, FUJIFILM, Wako, Osaka, Japan) at a dose of 150 mg/kg body weight.<sup>21</sup> The mice were considered diabetic when their nonfasting blood glucose levels exceeded 350 mg/dL for two consecutive daily readings.<sup>22</sup> Mice with nonfasting blood glucose levels greater than 600 mg/dL for two consecutive daily readings were selected as recipients. Blood glucose concentrations were determined using the glucose oxidase method (PocketChem BG PG-7320; Arkray, Kyoto, Japan).

### 2.2 | $^{111}\text{In}$ -exendin-4 synthesis and $^{111}\text{In}$ -exendin-4 accumulation in isolated islets

$^{111}\text{In}$ -exendin-4 probe was synthesized through a process involving isothiocyanate-benzyl-DTPA (BnDTPA) and 6-aminohexanoic acid (Ahx) attached to an  $\epsilon$ -amino group at the lysine-12 residue, as previously described.<sup>16</sup>  $^{111}\text{In}$ -exendin-4 accumulation was measured using isolated pancreatic islets of 8- to 10-week-old male C57BL/6JJmsSlc mice. Islets were isolated as previously described.<sup>22,23</sup> The islets were handpicked under a dissecting microscope.

After isolation, purified islets were cultured overnight in RPMI-1640 medium (catalog no. 186-02155; FUJIFILM, Wako, Osaka, Japan) containing 10% heat-inactivated fetal calf serum, 100 IU/mL penicillin, and 100 µg/mL streptomycin at 37°C in a humidified atmosphere (5% CO<sub>2</sub> and 95% air). After overnight recovery, islets were collected, counted, and transferred to tubes (50, 100, 200, 300, or 400 islets per tube,  $n = 11$ ). Approximately 0.37 MBq of <sup>111</sup>In exendin-4 was added, followed by incubation for 30 min on ice. The islets were washed using chilled phosphate-buffered saline, and radioactivity was measured in an auto-well  $\gamma$ -counter (Wallac 1480 WIZARD 3"  $\gamma$ -counter, PerkinElmer, Inc., Waltham, MA, USA), as previously described.<sup>24</sup> The results were expressed as radioisotope counts per minute from islets after 30 min of incubation.

### 2.3 | Islet transplantation and study design

The recipient mice were anesthetized using isoflurane. Before intraportal infusion, fresh islets were suspended in 500 µL of Hanks balanced salt solution (catalog no. H8264; Sigma-Aldrich). Based on previous reports, streptozotocin-induced diabetic mice (STZ-diabetic mice) were transplanted with 150 and 400 islets via the ileocecal vein.<sup>22,23</sup> Nonfasting blood glucose levels and body weights were measured every day for the first week after transplantation and once a week after that. The mice were divided into groups based on the number of transplanted islets and the success of engraftment as follows: (i) mice untreated with STZ and did not undergo islet transplantation (control), (ii) STZ-diabetic mice transplanted with 150 islets (150 IT), (iii) STZ-diabetic mice transplanted with 400 islets with successful engraftment (400 IT); and (iv) STZ-diabetic mice transplanted with 400 islets with unsuccessful engraftment (400\* IT). The successful engraftment in mice from the 400-islet-transplanted groups was defined with nonfasting blood glucose levels <200 mg/dL for two consecutive daily readings, which were maintained throughout the observation period.<sup>25</sup> The unsuccessful engraftment was considered in mice from the 400-islet-transplanted group with nonfasting blood glucose levels >350 mg/dL for two consecutive daily readings. The main comparisons involved the control, 150 IT, and 400 IT groups.

### 2.4 | Intraperitoneal glucose tolerance test

For the intraperitoneal glucose tolerance test (IPGTT), mice from the control, 150 IT, and 400 IT groups ( $n = 4$

for each group) were fasted for 16 h, then intraperitoneally administered 20% glucose solution (2 g/kg body weight). Blood samples were collected from the tail vein 0, 15, 30, 60, and 120 min after glucose administration. Insulin levels were measured using the Ultra Sensitive Mouse Insulin ELISA kit (catalog no. MS-303 (M1104); Morinaga Institute of Biological Science, Yokohama, Japan).

### 2.5 | Ex-vivo liver islet graft evaluation using the <sup>111</sup>In-exendin-4 probe

After a 6-week observation period following intraportal IT, mice from the control ( $n = 8$ ), 150 IT ( $n = 9$ ), 400 IT ( $n = 13$ ), and 400\* IT ( $n = 3$ ) groups were injected via the tail vein with <sup>111</sup>In-exendin-4 (3.0 MBq/mouse). The mice were sacrificed by cervical dislocation 30 min post-injection (p.i.), followed by immediate resection, weighing of the liver, and measurement of the radioactivity in the resected organ using an auto-well  $\gamma$ -counter. The liver graft uptake values were calculated by dividing the radioactivity from the organ by that of the total injection of the probe (<sup>111</sup>In exendin-4), normalized by dividing by the organ weight (%ID/g).<sup>17–20</sup>

### 2.6 | Liver graft insulin content and ex-vivo liver graft evaluation using the <sup>111</sup>In-exendin-4 probe

The mice were injected via the tail vein with <sup>111</sup>In exendin-4 (3.0 MBq/mouse) and sacrificed at 30 min p.i., followed by measurement of radioactivity in the resected organs using an auto-well  $\gamma$ -counter. The livers with islet grafts were cut and homogenized using the T-PER, Tissue Protein Extraction Reagent (catalog no 78510; Thermo Fisher Scientific, USA). After homogenization, the samples were centrifuged at 10000 rpm for 5 min, and the insulin levels of the supernatant were measured.

### 2.7 | In-vivo <sup>111</sup>In-exendin-4 SPECT/CT imaging

<sup>111</sup>In-exendin-4 SPECT/CT was performed in control ( $n = 4$ ), 150 IT ( $n = 3$ ), and 400 IT ( $n = 3$ ) groups 6 weeks after observation following intraportal IT. <sup>111</sup>In-exendin-4 (3.0 MBq/mouse) was injected via the tail vein, and SPECT/CT scanning was performed using a Triumph Lab PET12/SPECT4/CT (TriFoil Imaging Inc., Chatsworth, CA, USA) as previously described.<sup>17–20,26</sup> The cumulative sum of the liver and pancreas SPECT values was analyzed using Amira software, version 5.6.0 (FEI Visualization

Sciences Group, Düsseldorf, Germany). Based on previous reports,<sup>17–20,26</sup> the region of interest (ROI) was analyzed using images between the lower limit of the lung and the upper limit of the bladder. The pancreatic ROI was determined by comparing the outline of the pancreas on CT images; following that, a 2.7-mm region surrounding the kidney was excluded to avoid the huge potential influence of the kidneys on the signal intensity of the pancreas.<sup>17–20,26</sup> After determining the ROI of the kidneys and pancreas, the remaining abdominal signals were determined as the ROI of the liver grafts through comparison with the outline of the liver on CT images.

## 2.8 | Immunohistochemical analysis of BCM

Following SPECT/CT scans, the mice were sacrificed and subjected to immediate resection and weighing of the harvested livers. Tissues were immediately fixed in 10% buffered formalin phosphate at 4°C. For accurate quantification of BCM, 10 sets of serial formalin-fixed paraffin-embedded sections (4 µm per section; 100 µm between each set) were analyzed for each mouse, as previously reported.<sup>17–20,26</sup> The slides were incubated in blocking buffer supplemented with rabbit polyclonal anti-insulin primary antibody (100-fold dilution; catalog no. sc-9168; Santa Cruz Biotechnology, Santa Cruz, CA, USA), followed by a secondary antibody (Alexa Fluor 488 goat anti-rabbit antibody, 200-fold dilution; catalog no. A-11034; Thermo Fisher Scientific, USA). Adjacent sections were stained with hematoxylin and eosin. Stained tissue sections were observed under a fluorescence microscope (BZ-X700; Keyence, Osaka, Japan). The images were analyzed using BZ-II analyzer software (Keyence). The BCM was calculated from immunolabeled sections according to the formula: (insulin-positive area/whole tissue area) × tissue weight (mg).<sup>17,18</sup>

## 2.9 | Autoradiography

The recipient mice ( $n = 4$ ) were transplanted with 400 islets after 30 min of incubation in RPMI-1640 medium containing approximately 3.0 MBq <sup>111</sup>In exendin-4 via the ileocecal vein. The mice were sacrificed 24 h after the ITs and livers were immediately resected and frozen in liquid nitrogen. The 20-µm-thick fresh-frozen sections were immunostained with anti-insulin antibody as described above. The radioactivity and fluorescence images of the same sections were acquired using an image analyzer (Typhoon FLA 9500; GE Healthcare Bio-Sciences AB, Uppsala, Sweden) and a fluorescence microscope

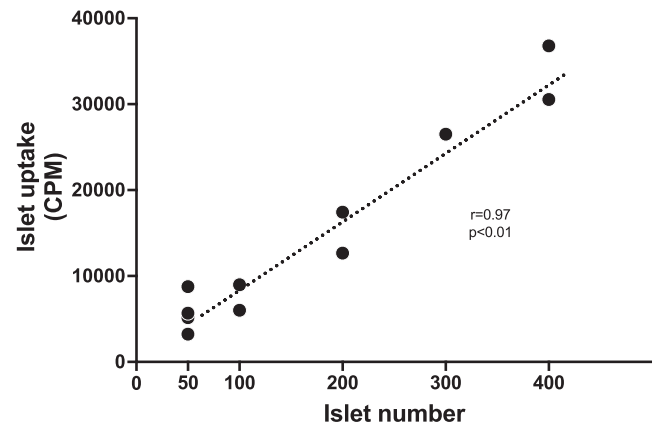


**FIGURE 1** <sup>111</sup>In-exendin-4 accumulation study in isolated pancreatic islets. Isolated islets (50, 100, 200, 300, and 400) from C57BL/6J mice were incubated with <sup>111</sup>In-exendin-4 for 30 min. A significant positive linear correlation was observed between <sup>111</sup>In-exendin-4 uptake values and the number of isolated islets (Pearson  $r = .97$ ,  $p < .01$ ).

(BZ-X700). Subsequently, the autoradiography study was performed in mice 2 weeks following intraportal IT. The mice were injected via the tail vein with <sup>111</sup>In exendin-4 (3.7 MBq/mouse), and livers were resected 30 min p.i. The radioactivity and fluorescence images of the same 20-µm-thick fresh-frozen liver sections were acquired as described above.

## 2.10 | Statistical analysis

All data are presented as mean ± SD. Statistical analyses were performed using a one-way analysis of variance with Turkey's multiple comparisons test and *Student's t-test* or *Mann-Whitney U test*. The Pearson correlation coefficient ( $r$ ) was used to analyze the correlations between two continuous variables. The level of significance was set at  $p < .05$ . Statistical analyses were performed using the GraphPad Prism 9 software (GraphPad Software, La Jolla, CA, USA).

## 3 | RESULTS

### 3.1 | <sup>111</sup>In-exendin-4 accumulation in isolated pancreatic islets correlated with the islet numbers

Isolated islets from C57BL/6JJmsSlc mice (ranging from 50 to 400 islets per tube) were incubated with 0.37 MBq of <sup>111</sup>In-exendin-4 for 30 min, and the relationship between the RI uptake and islet numbers was examined (Figure 1). A significant positive linear correlation was observed



between  $^{111}\text{In}$ -exendin-4 uptake values and the number of isolated islets ( $r = .97$ ,  $p < .01$ ).

### 3.2 | Intraportal transplantation of 400 islets restores normoglycemia in STZ-diabetic mice

The islet-transplanted mice were observed for 6 weeks following intraportal transplantation. Sixteen and nine STZ-diabetic mice were transplanted with 400 and 150 islets, respectively. Nonfasting blood glucose levels (600–800 mg/dL) measured on the day before transplantation did not significantly differ among the STZ-diabetic mice (Figure 2A). In the mice transplanted with 400 islets, the nonfasting blood glucose levels of 13 mice gradually decreased the day after transplantation and reached a level comparable to that of the control mice without STZ treatment or IT (blood glucose level  $< 200$  mg/dL) within 10–14 days after the transplantation, which met the criteria of successful engraftment (400 IT) (Figure 2A). However, three mice remained hyperglycemic throughout the observation period and met the criteria of unsuccessful engraftment (400\* IT). In the 150 IT group, the nonfasting blood glucose levels did not change significantly following transplantation. The body weight of all STZ-diabetic mice was not significantly different on the day before transplantation. The body weight gradually increased after IT, especially in the 400 IT group, while the body weight did not significantly differ among all the STZ-diabetic groups during the observation (Figure 2B). In addition, an IPGTT

was performed on the control, 150 IT, and 400 IT groups 6 weeks after IT ( $n = 4$  for each group, Figure S1). The blood glucose levels were not significantly different between the control and 400 IT groups, whereas the 150 IT group showed significantly higher plasma glucose levels at all time points than the control and 400 IT groups ( $p < .05$ ) (Figure S1A). The 150 IT group exhibited significantly lower insulin levels at 15 and 30 min after glucose administration than the control and 400 IT groups ( $p < .05$ ) (Figure S1A). The AUC<sub>0–30 min</sub> for insulin was significantly higher in the 400 IT group compared to the 150 IT group ( $p < .01$ ), although the AUC<sub>0–30 min</sub> in the 400 IT group was significantly smaller than that in the control group ( $p < .05$ ) (Figure S1B).

### 3.3 | Ex-vivo liver graft uptake of $^{111}\text{In}$ -exendin-4 was significantly higher in 400-islet-transplanted mice than in control and 150-islet-transplanted mice

Ex-vivo liver graft evaluation using  $^{111}\text{In}$  exendin-4 was performed 6 weeks after IT. The  $^{111}\text{In}$ -exendin-4 uptake in the resected livers from the 400 IT group was the highest among the four groups (Figure 2C). Uptake in the 400 IT group was significantly higher than in control and 150 IT groups ( $p < .0001$  and  $p < .001$ , respectively). Uptake in the 150 IT group tended to be higher than that in the control group, although there were no significant differences between the two groups. Notably, the ex-vivo liver graft uptake in the 400 IT group, which

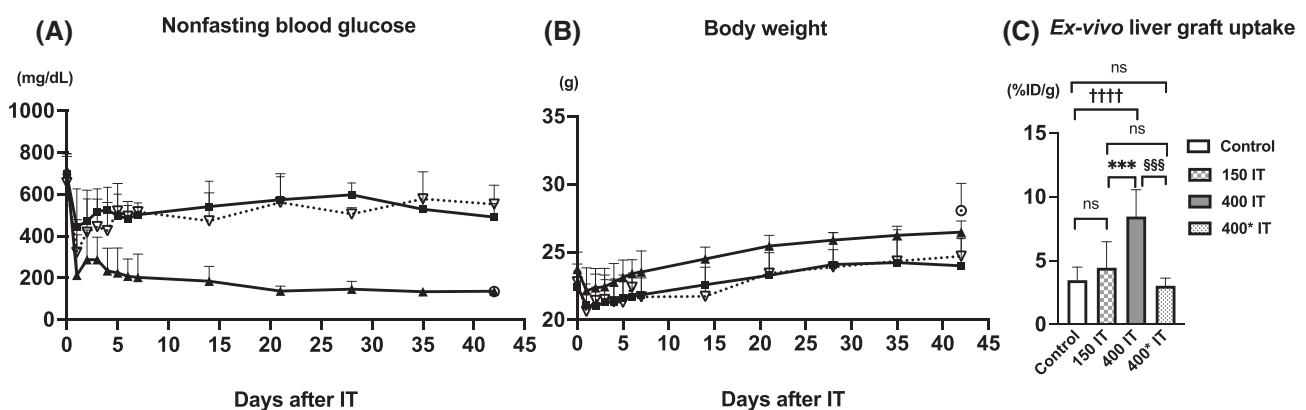


**FIGURE 2** Metabolic measurements after intraportal islet transplantation and ex-vivo liver graft uptake of the  $^{111}\text{In}$ -exendin-4 probe. (A) Nonfasting blood glucose and (B) body weight during the observation period. (C) Ex-vivo liver graft uptake (%ID/g) using  $^{111}\text{In}$ -exendin-4 probe 6 weeks following islet transplantation. All data are expressed as the mean  $\pm$  SD. Control is indicated as open circles with a dotted line and white bars with solid borders ( $n = 8$ ), 150 IT are indicated as closed squares with a solid line and checked bars with solid borders ( $n = 9$ ), and 400 IT with successful engraftment are indicated as closed triangles with a solid line, as well as gray bars with solid borders ( $n = 13$ ) and 400\* IT with unsuccessful engraftment are indicated as open triangles with a dotted line and dotted bars with solid borders ( $n = 3$ ). 400 IT versus control:  $++++p < .0001$ , 400 IT versus 150 IT:  $***p < .001$ , 400 IT versus 400\* IT:  $$$$p < .001$ . IT, islet transplantation; n.s., not significant.

met the criteria for successful engraftment, was significantly higher than that in the 400\* IT group, which did not meet the criteria for successful engraftment ( $p < .001$ ). The uptake in the 400\* IT group was not significantly different from that in the 150 IT group. The ex-vivo liver graft uptake results were consistent with the glycemic consequences in STZ-diabetic mice after IT (Figure 2A,C).

### 3.4 | Ex-vivo liver graft uptake of $^{111}\text{In}$ -exendin-4 was corroborated by the liver graft insulin content

The four control and four 150 IT mice, as well as the eight mice that underwent intraportal IT with 400 islets and resulted in the six 400 IT and two 400\* IT mice, were compared with respect to liver graft insulin content and ex-vivo liver graft uptake of  $^{111}\text{In}$ -exendin-4. As shown in Figure 3A, the 400 IT group exhibited the highest liver graft insulin levels among the four groups. The liver graft insulin levels in the 400 IT group were significantly higher than those in the 150 IT group (400 IT vs. 150 IT,  $0.676 \pm 0.240$  mg/g vs.  $0.025 \pm 0.025$  mg/g  $p < .001$ ), whereas insulin was not detected in the liver of the control group (400 IT vs. control,  $p < .001$ ). Moreover, the 400 IT group showed higher insulin levels than the 400\* IT group (400\* IT;  $0.008 \pm 0.003$  mg/g), similar to the 150 IT group. Consistent with the liver graft insulin content, the ex-vivo liver graft uptake of  $^{111}\text{In}$ -exendin-4 in the 400 IT group was the highest among the four groups (Figure 3B). Ex-vivo liver graft uptake in the 400 IT group was significantly higher than that in the 150

IT ( $p < .01$ ) and control ( $p < .001$ ) groups. Moreover, the 400 IT group showed higher ex-vivo liver graft uptake than the 400\* IT group, which was similar to that of the 150 IT group. The ex-vivo uptake of  $^{111}\text{In}$ -exendin-4 (Figure 3C) in the pancreas of the control group was comparable to that observed in previous reports.<sup>14,16,19</sup> The pancreatic uptake in the control group was significantly higher than that in the other STZ-diabetic mice, including the 150 IT ( $p < .0001$ ) and 400 IT ( $p < .0001$ ) groups (Figure 3C). These results demonstrated the ability to quantify  $\beta$ -cell specific uptake in the pancreas using the  $^{111}\text{In}$ -exendin-4 probe, as demonstrated in previous reports.<sup>17–21</sup>

### 3.5 | $^{111}\text{In}$ -exendin-4 SPECT/CT successfully visualized liver islet grafts in-vivo and showed significantly higher uptake in liver grafts of the 400 islet-transplanted mice than in control and 150 islet-transplanted mice

In-vivo  $^{111}\text{In}$ -exendin-4 SPECT/CT scans were performed on mice from the control, 150 IT, and 400 IT groups 6 weeks after IT. Representative SPECT/CT images for each group of mice are shown in Figure 4A. Whereas almost no intense signals in the liver for the SPECT/CT images were observed in the control group, a few weak-intensity signals in the liver were observed in the 150 IT group and a more significant number of higher-intensity signals were observed in the 400 IT group. With respect to the pancreas,  $^{111}\text{In}$ -exendin-4 SPECT/CT exhibited a higher uptake in the

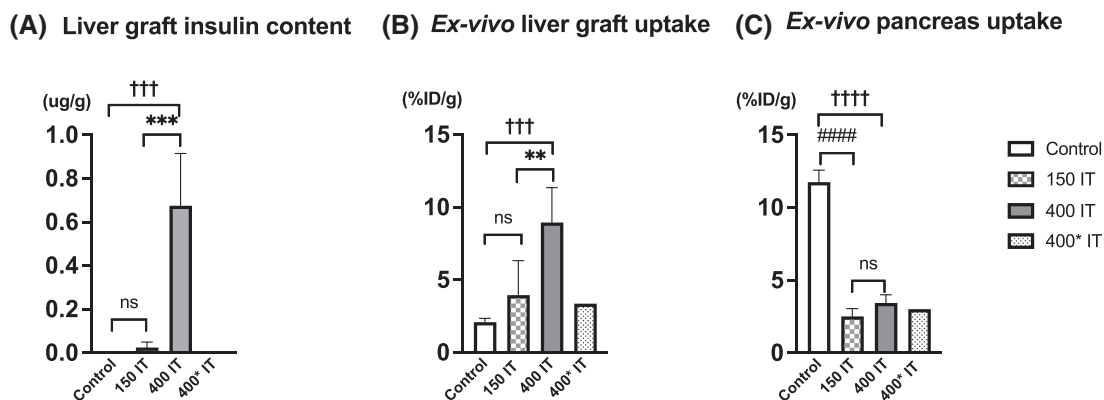


**FIGURE 3** Liver graft insulin content and ex-vivo liver graft and pancreas uptake of  $^{111}\text{In}$ -exendin-4 6 weeks after islet transplantation. (A) Liver graft insulin content, (B) ex-vivo liver uptake, and (C) ex-vivo pancreas uptake (%ID/g) using the  $^{111}\text{In}$ -exendin-4 probe. All data are expressed as the mean  $\pm$  SD. Control is indicated as white bars with solid borders ( $n = 4$ ), 150 IT are indicated as checked bars with solid borders ( $n = 4$ ), and 400 IT with successful engraftment are indicated as gray bars with solid borders ( $n = 6$ ) and 400\* IT with unsuccessful engraftment are indicated as dotted bars with solid borders ( $n = 2$ ). 400 IT versus control:  $^{\dagger\dagger\dagger}p < .001$ ,  $^{\dagger\dagger\dagger\dagger}p < .0001$ ; 400 IT versus 150 IT:  $^{**}p < .01$ ,  $^{***}p < .001$ ; 150 IT versus control:  $^{####}p < .0001$ . IT, islet transplantation; n.s., not significant.

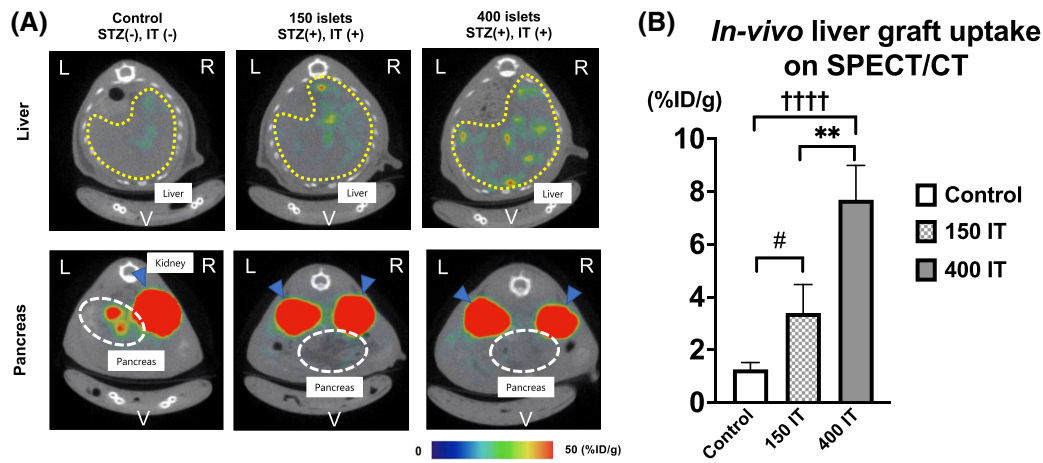


**FIGURE 4** Representative images of in-vivo  $^{111}\text{In}$ -exendin-4 SPECT/CT and in-vivo liver graft uptake after islet transplantation. (A) In-vivo  $^{111}\text{In}$ -exendin-4 SPECT/CT was performed 6 weeks after islet transplantation in control, 150 IT, and 400 IT groups. Signals from the graft in the liver, yellow dashed circles; pancreas, white dashed circles; and signals from the kidney, blue arrows. L—left; R—right; V—ventral. (B) In-vivo liver graft  $^{111}\text{In}$ -exendin-4 uptake (%ID/g) detected by SPECT/CT. Data are expressed as the mean  $\pm$  SD. 400 IT versus control:  $^{++++}p < .0001$ ; 400 IT versus 150 IT:  $^{**}p < .01$ ; 150 IT versus control:  $^{\#}p < .05$ . IT, islet transplantation.

control group than in the STZ-diabetic 150 IT and 400 IT groups. The  $^{111}\text{In}$ -exendin-4 SPECT/CT images revealed distinct in-vivo liver graft uptake among the IT groups. The values for the 400 IT group were significantly higher than those for the control ( $p < .0001$ ) and 150 IT ( $p < .01$ ) groups (Figure 4B), which was consistent with the ex-vivo liver graft uptake data (Figure 3B).

### 3.6 | In-vivo liver graft uptake in $^{111}\text{In}$ -exendin-4 SPECT/CT images was corroborated by and showed a significant correlation with the histologically analyzed liver graft BCM

Conventional histological analyses of the islet graft BCM in the liver samples were performed. The islet grafts were found scattered throughout the liver lobes and were located mainly around the perivascular areas in the IT groups (Figure 5A). More insulin-positive islets were observed in the 400 IT group compared with that in the 150 IT group (Figure 5A). The liver graft BCM was significantly larger in the 400 IT group than in control ( $p < .001$ ) and 150 IT ( $p < .001$ ) groups (Figures 5B), which corroborated the results of the in-vivo liver graft uptake in  $^{111}\text{In}$ -exendin-4 SPECT/CT (Figure 4B). Notably, a statistically significant correlation was observed between in-vivo liver graft uptake in  $^{111}\text{In}$ -exendin-4 SPECT/CT and the histologically calculated liver graft BCM ( $r = .95$ ;  $p < .01$ ; Figure 5C).

### 3.7 | Autoradiographic signals were colocalized with fluorescence signals of islet grafts

Autoradiography study demonstrated radioactive signals colocalized with fluorescence signals of islet grafts in the liver of the mice in which intraportal IT was performed after the islet incubation with  $^{111}\text{In}$  exendin-4 (Figure 6A). In addition, colocalization between radioactive signals and fluorescent images of the islet grafts was also confirmed in the liver of the mice in which  $^{111}\text{In}$  exendin-4 was injected via the tail vein following intraportal IT (Figure 6B).

## 4 | DISCUSSION

In the present study, we evaluated the use of  $^{111}\text{In}$ -exendin-4 SPECT/CT for noninvasive visualization of islet grafts and determined the BCM following intraportal transplantation. Incubation of isolated mouse islets with  $^{111}\text{In}$ -exendin-4 indicated that  $^{111}\text{In}$ -exendin-4 accumulation was significantly correlated with the number of isolated islets. Six weeks after intraportal IT, ex-vivo  $^{111}\text{In}$ -exendin-4 liver graft uptake in the 400 IT group was considerably higher than in control and 150 IT groups, consistent with the in-vivo glycemic consequences and liver graft insulin levels. Furthermore, in-vivo  $^{111}\text{In}$ -exendin-4 SPECT/CT displayed liver islet grafts and distinguished the control, 150 IT, and 400 IT mice, in which  $^{111}\text{In}$ -exendin-4 uptake in the liver was significantly correlated with the

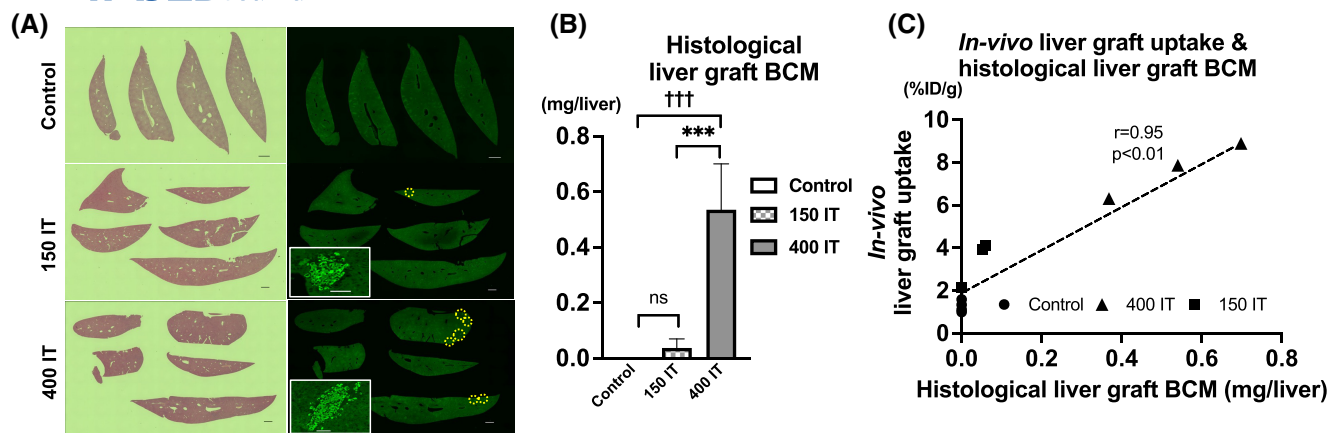


**FIGURE 5** Histological liver graft  $\beta$ -cell mass after islet transplantation and its correlation with in-vivo  $^{111}\text{In}$ -exendin-4 SPECT/CT liver graft uptake. (A) Representative images of hematoxylin and eosin staining (left panel) and immunohistochemical anti-insulin staining (right panel) on the serial liver sections. Scale bars: 1000  $\mu\text{m}$  in the overview images and 50  $\mu\text{m}$  in the high-magnification images. (B) Liver graft  $\beta$ -cell mass (BCM) as calculated by histological analysis. Data are expressed as the mean  $\pm$  SD. Control is indicated as white bars with solid borders ( $n = 4$ ). 150 IT are indicated as checked bars with solid borders ( $n = 3$ ). 400 IT with successful engraftment are indicated as gray bars with solid borders ( $n = 3$ ). 400 IT versus control:  $^{\dagger\dagger\dagger}p < .001$ ; 400 IT versus 150 IT:  $^{***}p < .001$ ; 150 IT versus control: n.s., not significant. (C) Significant correlation between liver graft uptake values on  $^{111}\text{In}$ -exendin-4 SPECT/CT (percentage of injected dose/1 g, %ID/g) and histological quantification of BCM (Pearson  $r = .95$ ,  $p < .01$ ). IT, islet transplantation.

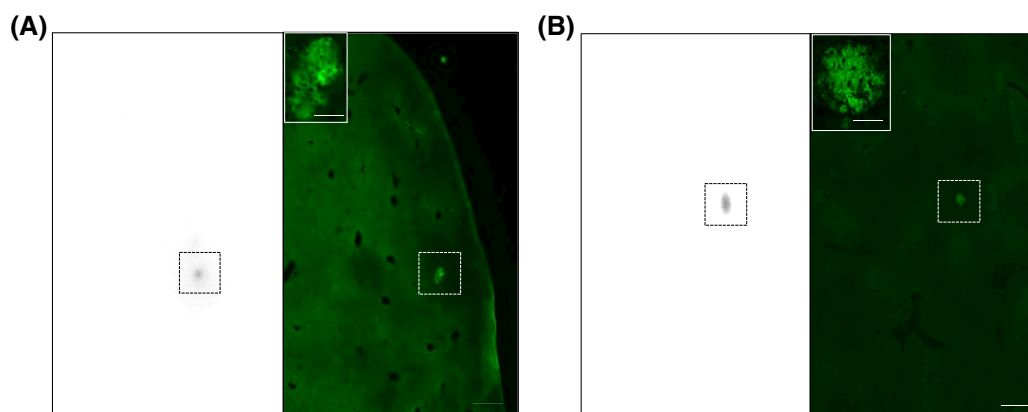


**FIGURE 6** Representative autoradiography and corresponding fluorescence images on the liver islet grafts. (A) Autoradiography (left panel) and fluorescence microscopy image with anti-insulin staining (right panel) on the same liver graft section, which was harvested from the mice transplanted with islets after incubation with  $^{111}\text{In}$  exendin-4. (B) Autoradiography (left panel) and fluorescence microscopy image with anti-insulin staining (right panel) on the same liver graft section, harvested from the mice in which  $^{111}\text{In}$  exendin-4 was injected via the tail vein following intraportal IT. Radioactive signals colocalized with the fluorescence signals of islet grafts (dashed-line boxes). Box: high-magnification image of the insulin-positive area. Scale bar: 200  $\mu\text{m}$  in the overview images and 50  $\mu\text{m}$  in the high-magnification images.

histological analysis of liver graft BCM. In addition, the autoradiography study showed colocalization of radioactive and fluorescence signals of the islet grafts of the liver in IT mice. These findings suggest that  $^{111}\text{In}$ -exendin-4 SPECT/CT may be useful for the noninvasive evaluation of islet graft BCM after intraportal transplantation.

Direct assessments of islet graft BCM remain challenging in current clinical evaluations of transplantation efficacies.<sup>12,13</sup> Recently, the development of exendin-based GLP-1R-targeted  $\beta$ -cell imaging has shed light on this issue.<sup>4,13,14</sup> However, most studies involving such

imaging have focused on insulinoma or the pancreas alone,<sup>16,24,27–29</sup> whereas only a limited number of studies have examined the possibility of islet graft evaluation for IT. Eter et al. reported that  $^{111}\text{In}$ -exendin-3 SPECT/CT displayed islet grafts in intramuscular IT mice, and the uptake in calf muscle correlated with graft volume<sup>30,31</sup>; however, muscle is not favorable in IT and intramuscular transplantation remains very uncommon in the clinic. The  $^{111}\text{In}$ -exendin-3 uptake in the background liver is reasonably higher compared with those in muscle, and intraportal islet grafts have not been examined by  $^{111}\text{In}$ -exendin-3



SPECT/CT. Moreover, exendin-3 probes indicate the need to improve stability compared with exendin-4.<sup>14,29</sup> Thus, interpreting the results with <sup>111</sup>In-exendin-3 remains difficult for intraportal IT and clinical applications. Therefore, we employed a <sup>111</sup>In-exendin-4 probe and SPECT/CT for intraportal IT model mice, in which in-vivo liver graft uptake in <sup>111</sup>In-exendin-4 SPECT/CT, as well as ex-vivo liver graft uptake, could distinguish mice with different numbers of intraportally transplanted islets and glycemic consequences (Figures 2 and 4B).

Other reports regarding exendin-based GLP-1R-targeted imaging for islet graft evaluation included iron-oxide-labeled exendin-4 magnetic resonance imaging.<sup>32,33</sup> Although prelabeled islets with superparamagnetic iron oxide (SPIO) can be tracked in mice with kidney capsular IT and intraportal IT-received patients with type 1 diabetes,<sup>34–36</sup> the SPIO signal is not specific to  $\beta$ -cells and shows persistent deposition even after loss or destruction of the viable islet grafts.<sup>12,34–36</sup> While manganese magnetism-engineered iron oxide nanoparticles with exendin-4 improved  $\beta$ -cell specificity, the need for pre-labeling hampers repeated real-time observations of islet grafts and a large amount of iron content in the liver results in a low quantitative capability of the probe.<sup>32,33</sup> Based on these points, the <sup>111</sup>In-exendin-4 probe avoids pre-labeling graft islets and allows repeated intravenous administration for in-vivo observation.<sup>14,17–21</sup> Moreover, <sup>111</sup>In-exendin-4 accumulation in islet grafts was corroborated by liver insulin content (Figure 3A,B), which suggests that <sup>111</sup>In-exendin-4 signals reflect viable rather than destroyed islets. The quantitative capability of islet graft BCM by <sup>111</sup>In-exendin-4 was demonstrated in in-vivo and ex-vivo comparisons of liver graft uptake in the mice transplanted with different islet numbers (Figures 2C and 4B), along with the finding that in-vivo liver graft uptake was significantly correlated with histological liver graft BCM (Figure 5C).

This study had several limitations. The number of mice used for the in-vivo SPECT/CT analysis was relatively small because using the same lot of <sup>111</sup>In-exendin-4 probe limited the number of scanned mice per day, which may have prevented a robust conclusion regarding the potential of <sup>111</sup>In-exendin-4 SPECT/CT in tracking subtle differences of islet graft BCM. Moreover, ex-vivo liver graft uptake of the <sup>111</sup>In-exendin-4 probe did not show a significant difference between the control and 150 IT mice, although the uptake in 150 IT mice tended to be higher than that in the control mice. It should also be noted that histological liver graft BCM did not show significant differences between the control and 150 IT mice, consistent with the results of ex-vivo liver graft uptakes. The scattered islets throughout the whole liver may have hampered the counts for full transplant in histological samples. Although there were significant differences in

liver graft uptake in-vivo and ex-vivo between the 400 IT and the control/150 IT mice, and the significant correlation between in-vivo liver graft uptake and histological liver graft BCM in all groups indicates the potential of the <sup>111</sup>In exendin-4 probe for quantifying islet graft BCM. The limited spatial resolution of SPECT may become an obstacle to better quantitation.<sup>14,37</sup> Consequently, utilizing PET may offer better spatial resolution and improve the detection and quantitation of islet grafts.<sup>14,24,27</sup> Although a recent report using <sup>18</sup>F-tetrazine trans-cyclooctene-Cys(40)-exendin-4 PET showed high background signals in the liver and did not yield sufficient specificity for islet grafts in intraportal IT mice,<sup>38</sup> our exendin-4-based probe may be promising due to the reasonably low background signals.<sup>24,27</sup> In this study, comparisons of <sup>111</sup>In exendin-4 SPECT/CT with other imaging techniques or current clinical methods were not included. Thus, further studies on noninvasive techniques for visualizing and quantifying transplanted islets are warranted to reveal the merit of different imaging approaches and conventional methods that assess the clinical outcomes of IT. Finally, longitudinal evaluation of graft BCM should be considered for further exploration of the utility of <sup>111</sup>In-exendin-4 SPECT/CT; this study focused on fundamental data of <sup>111</sup>In exendin-4 for visualization and quantification of liver graft BCM based on cross-sectional comparative observations. In-vivo liver graft uptake measurements before and after alloxan treatment might be helpful to further validate the noninvasive quantification of viable graft BCM by this method and provide additional evidence for the utility in the field of intraportal islet transplantation.

In summary, we demonstrated that <sup>111</sup>In-exendin-4 SPECT/CT could display islet grafts in the liver noninvasively in intraportal IT mice. <sup>111</sup>In-exendin-4 uptake in the liver was corroborated with glycemic outcome and liver insulin content. Furthermore, <sup>111</sup>In-exendin-4 uptake in the liver correlated with histologically analyzed liver graft BCM. Therefore, <sup>111</sup>In-exendin-4 SPECT/CT may be useful for quantifying islet graft BCM. These findings open new possibilities to provide real-time quantitative information on viable islet grafts noninvasively during intraportal IT follow-up.

## AUTHOR CONTRIBUTIONS

Ainur Botagarova and Takaaki Murakami planned the study; acquired and analyzed the data; and wrote, reviewed, and edited the manuscript. Hiroyuki Fujimoto contributed to the discussion. Nanae Fujimoto, Muhammad Fauzi, Sakura Kiyobayashi, and Daisuke Otani contributed to the data acquisition. Nobuya Inagaki supervised the research, contributed to the discussion, and reviewed the manuscript. All the authors have reviewed the results and approved the final version of the manuscript.

## ACKNOWLEDGMENTS

The authors thank Takashi Nishimoto and Norinaga Kakishita (Radioisotope Research Center, Kyoto University) for assistance with the radioisotope study and SPECT/CT scan.

## FUNDING INFORMATION

This study was supported by grants from the Ministry of Education, Culture, Sports, Science and Technology (MEXT), the Japan Society for the Promotion of Science (JSPS) (grant numbers 21K20931, 21K08553, and 22K16411), the Japan Association for Diabetes Education and Care, Japan Diabetes Foundation, the Japan Foundation for Applied Enzymology (Front Runner of Future Diabetes Research), and the Japan IDDM network.

## DISCLOSURES

N.I. received joint research grants from Daiichi Sankyo Co., Ltd., Terumo Co., Ltd., and Drawbridge Health, Inc.; received speaker honoraria from Kowa Pharmaceutical Co., Ltd., MSD, Astellas Pharma Inc., Novo Nordisk Pharma Ltd., Ono Pharmaceutical Co., Ltd., Nippon Boehringer Ingelheim Co., Ltd., Takeda Pharmaceutical Co., Ltd., and Mitsubishi Tanabe Pharma Co., Ltd.; received scholarship grants from Kissei Pharmaceutical Co., Ltd., Sanofi, Daiichi-Sankyo Co., Ltd., Mitsubishi Tanabe Pharma Co., Ltd., Takeda Pharmaceutical Co., Ltd., Japan Tobacco Inc., Kyowa Kirin Co., Sumitomo Pharma Co., Ltd., Astellas Pharma Inc., MSD, Eli Lilly Japan, Ono Pharmaceutical Co., Ltd., Sanwa Kagaku Kenkyusho Co. Ltd., Nippon Boehringer Ingelheim Co., Ltd., Novo Nordisk Pharma Ltd., Novartis Pharma K.K., Teijin Pharma Ltd., and Life Scan Japan Inc. The remaining authors have no conflicts of interest to declare.

## DATA AVAILABILITY STATEMENT

The data supporting this study's findings are available in this article's Material and Methods and Supporting Information.

## ORCID

Ainur Botagarova  <https://orcid.org/0000-0001-5610-4659>

Takaaki Murakami  <https://orcid.org/0000-0003-3844-1138>

## REFERENCES

- Meier JJ. Beta cell mass in diabetes: a realistic therapeutic target? *Diabetologia*. 2008;51(5):703-713. doi:10.1007/s00125-008-0936-9
- Powers AC. Type 1 diabetes mellitus: much progress, many opportunities. *J Clin Invest*. 2021;131(8):e142242. doi:10.1172/JCI142242
- Nakamura T, Fujikura J, Inagaki N. Advancements in transplantation therapy for diabetes: pancreas, islet and stem cell. *J Diabetes Investig*. 2020;12(2):143-145. doi:10.1111/jdi.13358
- Sakurai T, Kubota S, Kato T, Yabe D. Advances in insulin therapy from discovery to  $\beta$ -cell replacement. *J Diabetes Investig*. 2022;14:15-18. doi:10.1111/jdi.13902
- Shapiro AMJ, Lakey JRT, Ryan EA, et al. Islet transplantation in seven patients with type 1 diabetes mellitus using a glucocorticoid-free immunosuppressive regimen. *N Engl J Med*. 2000;343(4):230-238. doi:10.1056/NEJM200007273430401
- Marfil-Garza BA, Imes S, Verhoeff K, et al. Pancreatic islet transplantation in type 1 diabetes: 20-year experience from a single-Centre cohort in Canada. *Lancet Diabetes Endocrinol*. 2022;10(7):519-532. doi:10.1016/S2213-8587(22)00114-0
- Shapiro AMJ, Ricordi C, Hering BJ, et al. International trial of the Edmonton protocol for islet transplantation. *N Engl J Med*. 2006;355(13):1318-1330. doi:10.1056/NEJMoa061267
- Ryan EA, Paty BW, Senior PA, et al. Five-year follow-up after clinical islet transplantation. *Diabetes*. 2005;54(7):2060-2069. doi:10.2337/diabetes.54.7.2060
- Yamada Y, Fukuda K, Fujimoto S, et al. SUIT, secretory units of islets in transplantation: an index for therapeutic management of islet transplanted patients and its application to type 2 diabetes. *Diabetes Res Clin Pract*. 2006;74(3):222-226. doi:10.1016/j.diabres.2006.03.030
- Shapiro AMJ, Hao EG, Lakey JRT, et al. Novel approaches toward early diagnosis of islet allograft rejection. *Transplantation*. 2001;71(12):1709-1718. doi:10.1097/00007890-200106270-00002
- Oram RA, Sims EK, Evans-Molina C. Beta cells in type 1 diabetes: mass and function; sleeping or dead? *Diabetologia*. 2019;62:567-577. doi:10.1007/s00125-019-4822-4
- Arifin DR, Bulte JWM. In vivo imaging of pancreatic islet grafts in diabetes treatment. *Front Endocrinol*. 2021;12:640117. doi:10.3389/fendo.2021.640117
- Tiedge M. Inside the pancreas: progress and challenges of human beta cell mass quantification. *Diabetologia*. 2014;57(5):856-859. doi:10.1007/s00125-014-3206-z
- Murakami T, Fujimoto H, Inagaki N. Non-invasive beta-cell imaging: visualisation, quantification, and beyond. *Front Endocrinol*. 2021;12:714348. doi:10.3389/fendo.2021.714348
- Brom M, Andrałojć K, Oyen WJ, Boerman OC, Gotthardt M. Development of radiotracers for the determination of the beta-cell mass in vivo. *Curr Pharm des*. 2010;16(14):1561-1567. doi:10.2174/138161210791164126
- Kimura H, Fujita N, Kanbe K, et al. Synthesis and biological evaluation of an  $^{111}\text{In}$ -labeled exendin-4 derivative as a single-photon emission computed tomography probe for imaging pancreatic  $\beta$ -cells. *Bioorg Med Chem*. 2017;25(20):5772-5778. doi:10.1016/j.bmc.2017.09.005
- Murakami T, Fujimoto H, Fujita N, Hamamatsu K, Matsumoto K, Inagaki N. Noninvasive evaluation of GPR119 agonist effects on  $\beta$ -cell mass in diabetic male mice using  $^{111}\text{In}$ -Exendin-4 SPECT/CT. *Endocrinology*. 2019;160(12):2959-2968. doi:10.1210/en.2019-00556
- Fujita N, Fujimoto H, Hamamatsu K, et al. Noninvasive longitudinal quantification of  $\beta$ -cell mass with  $^{111}\text{In}$ -labeled exendin-4. *FASEB J*. 2019;33(11):11836-11844. doi:10.1096/fj.201900555R

19. Kiyobayashi S, Murakami T, Harada N, et al. Noninvasive evaluation of GIP effects on  $\beta$ -cell mass under high-fat diet. *Front Endocrinol.* 2022;13:921125. doi:10.3389/fendo.2022.921125
20. Fauzi M, Murakami T, Fujimoto H, et al. Preservation effect of imeglimin on pancreatic  $\beta$ -cell mass: noninvasive evaluation using  $^{111}\text{In}$ -exendin-4 SPECT/CT imaging and the perspective of mitochondrial involvements. *Front Endocrinol.* 2022;13:1010825. doi:10.3389/fendo.2022.1010825
21. Murakami T, Fujimoto H, Fujita N, Hamamatsu K, Yabe D, Inagaki N. Association of glucagon-like peptide-1 receptor-targeted imaging probe with in vivo glucagon-like peptide-1 receptor agonist glucose-lowering effects. *J Diabetes Investig.* 2020;11(6):1448-1456.
22. Yonekawa Y, Okitsu T, Wake K, et al. A new mouse model for intraportal islet transplantation with limited hepatic lobe as a graft site. *Transplantation.* 2006;82(5):712-715. doi:10.1097/01.tp.0000234906.29193.a6
23. Toyoda K, Okitsu T, Yamane S, et al. GLP-1 receptor signaling protects pancreatic beta cells in intraportal islet transplant by inhibiting apoptosis. *Biochem Biophys Res Commun.* 2008;367(4):793-798. doi:10.1016/j.bbrc.2008.01.046
24. Murakami T, Fujimoto H, Hamamatsu K, et al. Distinctive detection of insulinoma using  $^{18}\text{F}$ FB(ePEG12)12-exendin-4 PET/CT. *Sci Rep.* 2021;11(1):15014. doi:10.1038/s41598-021-94595-6
25. Li F, Jiao A, Li X, Zhang C, Sun N, Zhang J. Survival and metabolic function of syngeneic mouse islet grafts transplanted into the hepatic sinus tract. *Transplantation.* 2018;102(11):1850-1856. doi:10.1097/TP.0000000000002289
26. Hamamatsu K, Fujimoto H, Fujita N, et al. Establishment of a method for in-vivo SPECT/CT imaging analysis of  $^{111}\text{In}$ -labeled exendin-4 pancreatic uptake in mice without the need for nephrectomy or a secondary probe. *Nucl Med Biol.* 2018;64-65:22-27. doi:10.1016/j.nucmedbio.2018.06.002
27. Fujimoto H, Fujita N, Hamamatsu K, et al. First-in-human evaluation of positron emission tomography/computed tomography with  $^{18}\text{F}$ FB(ePEG12)12-exendin-4: a phase 1 clinical study targeting GLP-1 receptor expression cells in pancreas. *Front Endocrinol (Lausanne).* 2021;12:717101. doi:10.3389/fendo.2021.717101
28. Brom M, Joosten L, Frielink C, Boerman O, Gotthardt M.  $^{111}\text{In}$ -exendin uptake in the pancreas correlates with the  $\beta$ -cell mass and not with the  $\alpha$ -cell mass. *Diabetes.* 2015;64(4):1324-1328. doi:10.2337/db14-1212
29. Velikyan I, Eriksson O. Advances in GLP-1 receptor targeting radiolabeled agent development and prospective of theranostics. *Theranostics.* 2020;10(1):437-461. doi:10.7150/thno.38366
30. Eter WA, Van der Kroon I, Andralojc K, et al. Non-invasive in vivo determination of viable islet graft volume by  $^{111}\text{In}$ -exendin-3. *Sci Rep.* 2017;7(1):7232. doi:10.1038/s41598-017-07815-3
31. Van der Kroon I, Andralojc K, Willekens SM, et al. Noninvasive imaging of islet transplants with  $^{111}\text{In}$ -Exendin-3 SPECT/CT. *J Nucl Med.* 2016;57(5):799-804. doi:10.2967/jnumed.115.166330
32. Juang JH, Shen CR, Wang JJ, et al. Exendin-4-conjugated manganese magnetism-engineered iron oxide nanoparticles as a potential magnetic resonance imaging contrast agent for tracking transplanted  $\beta$ -cells. *Nanomaterials (Basel).* 2021;11(11):3145. doi:10.3390/nano11113145
33. Juang JH, Wang JJ, Shen CR, et al. Magnetic resonance imaging of transplanted porcine neonatal pancreatic cell clusters labeled with exendin-4-conjugated manganese magnetism-engineered iron oxide nanoparticles. *Nanomaterials (Basel).* 2022;12(7):1222. doi:10.3390/nano12071222
34. Juang JH, Shen CR, Wang JJ, et al. Magnetic resonance imaging of mouse islet grafts labeled with novel chitosan-coated superparamagnetic iron oxide nanoparticles. *PLOS One.* 2013;8(4):e62626. doi:10.1371/journal.pone.0062626
35. Toso C, Vallee JP, Morel P, et al. Clinical magnetic resonance imaging of pancreatic islet grafts after iron nanoparticle labeling. *Am J Transplant.* 2008;8(3):701-706. doi:10.1111/j.1600-6143.2007.02120.x
36. Saudek F, Jiráček D, Girman P, et al. Magnetic resonance imaging of pancreatic islets transplanted into the liver in humans. *Transplantation.* 2010;90(12):1602-1606. doi:10.1097/tp.0b013e3181ffba5e
37. Khalil MM, Tremoleda JL, Bayomy TB, Gsell W. Molecular SPECT imaging: an overview. *Int J Mol Imaging.* 2011;2011:796025. doi:10.1155/2011/796025
38. Wu Z, Liu S, Hassink M, et al. Development and evaluation of  $^{18}\text{F}$ -TTCO-Cys40-Exendin-4: a PET probe for imaging transplanted islets. *J Nucl Med.* 2013;54(2):244-251. doi:10.2967/jnumed.112.109694

## SUPPORTING INFORMATION

Additional supporting information can be found online in the Supporting Information section at the end of this article.

**How to cite this article:** Botagarova A, Murakami T, Fujimoto H, et al. Noninvasive quantitative evaluation of viable islet grafts using  $^{111}\text{In}$ -exendin-4 SPECT/CT. *The FASEB Journal.* 2023;37:e22859. doi:10.1096/fj.202201787RR